

Change of ζ Potential of Biocompatible Colloidal Oxide Particles upon Adsorption of Bovine Serum Albumin and Lysozyme

K. Rezwan,* A. R. Studart, J. Vörös, and L. J. Gauckler

Nonmetallic Inorganic Materials, Department Materials, ETH Zurich, Switzerland

Received: January 31, 2005; In Final Form: June 7, 2005

The amounts of negatively charged bovine serum albumin and positively charged lysozyme adsorbed on alumina, silica, titania, and zirconia particles (diameters 73 to 271 nm) in aqueous suspensions are measured. The adsorbed proteins change the ζ potentials and the isoelectric points (IEP) of the oxide particles. The added to adsorbed protein ratios at pH 7.5 are compared with the protein treated particle ζ potentials. It is found that the amounts of adsorbed proteins on the alumina, silica, and titania (but not on the zirconia) particle surfaces are highly correlated with the ζ potential. For the slightly less hydrophilic zirconia particles high amounts of protein adsorption are observed even under repulsive electrostatic conditions. One reason could be that the hydrophobic effect plays a more important role for zirconia than electrostatic interaction.

1. Introduction

Protein adsorption and desorption on planar material surfaces have been investigated in detail over the past few years by in situ techniques such as ellipsometry, optical waveguide light mode spectroscopy (OWLS), and quartz crystal microbalance (QCM).¹ Despite their usefulness in providing quantitative data on protein adsorption, the optical and the QCM methods lack direct information about surface potential and charge, which are known to strongly affect protein adhesion and conformation at interfaces.^{2–8} Streaming potential measurements can be used as a tool to characterize the surface potential of proteins interacting with planar surfaces⁹ but rarely have been used to characterize protein interfaces. Adsorption of proteins in aqueous particle systems has been investigated extensively in earlier studies.^{10–13}

In this paper we present a systematic investigation of the protein adsorption on various ceramic particles with a special focus on the influence of the particle surface charge and the adsorbed amount of proteins.

Positively charged lysozyme (LSZ) and negatively charged bovine serum albumin (BSA) were adsorbed to alumina, silica, titania, and zirconia colloidal particles with diameters ranging from 73 to 271 nm. The influence on the ζ potential and the isoelectric point (IEP) was monitored and correlated with the protein amounts adsorbed. These oxides were chosen as they are the main ceramic surfaces which are present in today's biomaterials¹⁴ and are of interest for a variety of life science applications.

2. Experimental Section

2.1. Materials. *2.1.1. Oxide Particles.* Amorphous SiO₂ (Snowtex ZL, Lot 140828) was obtained from Nissan Chemicals Industries Ltd as a 30 vol % suspension. To lower the salt content, the suspension was dialyzed for a few days using a dialysis tube (ZelluTrans ROTH) until the electrical conductivity

fell below 1 μ S/cm. TiO₂ anatase was obtained from Kronos (Kronos 1171, Lot 60082–60083) and washed by a procedure described elsewhere¹⁵ to remove the surface acidic groups originating from the powder production process. The washing process was controlled by ζ potential measurements and resulted in a shift of the isoelectric point from pH 2 to pH 5,¹⁶ indicating the removal of the acidic groups from the powder surface. α -Al₂O₃ was purchased from Taimei (TM-DAR, Lot 3973) and monoclinic ZrO₂ from Tosoh (TZ-0, Lot Z006288P).

All powders were of high purity grade (>99.99 wt %) and were calcined at 400 °C for 4 h to eliminate any organic residues. The specific surface areas of all powders were characterized by BET (Nova 1000 Series, Quantachrome). The surface tensions of 2 vol % oxide suspensions were measured by the drop pendant method (PAT 1, SINTERFACE).¹⁷ Particle size distributions were analyzed with an X-ray centrifuge sedigraph (XDC, Brookhaven Instruments) confirming that all powders were of narrow and monomodal distribution. The powder properties including their measured IEPs, surface tensions, and Hamaker constants^{18,19} are summarized in Table 1. Scanning electron micrographs of the particles documented their size and globular morphology.

Double deionized water with an electrical resistance of 18 M Ω cm from a NANOpure water system (Barnstead) was used for all experiments.

2.1.2. Proteins and Protein Reagent. Chicken hen egg white lysozyme (L6876, Lot 051K7028) and bovine serum albumin (A7906, Lot 12K1608) were purchased from Sigma Aldrich and used without any modifications. A SDS-PAGE analysis according to Laemmli²⁰ confirmed both protein lots being of high purity (>~98 wt %). The surface tensions of LSZ and BSA solutions of 2.5 mg/mL concentration were measured by the drop pendant method as well. Table 2 shows a comparison of the protein data of Lysozyme (LSZ) and Bovine Serum Albumin (BSA) taken from refs 21 and 22.

Bradford reagent²³ was used as a protein dye and was purchased from Sigma Aldrich (B6916, Lot. No. 52K9311).

2.2. Measurement Methods. *2.2.1. Preparation of the Oxide Suspensions and Protein Addition.* For each ζ potential measurement 50 mL of an oxide suspension with 2 vol % powder

* Address correspondence to this author. Nichtmetallische Werkstoffe, Wolfgang-Pauli-Strasse 10, ETH Hönggerberg, HCI G 538, 8093 Zürich. Phone: +41-1-632-68-53. Fax: +41-1-632-11-32. E-mail: kurosch.rezwan@mat.ethz.ch.

TABLE 1: Physical Properties of Oxide Particles Used^a

	SiO ₂	Al ₂ O ₃	TiO ₂	ZrO ₂
crystal structure	amorphous	alpha	anatase	monoclinic
density [g/cm ³]	1.95	3.98	3.80	5.82
diameter (<i>d</i> ₅₀) [nm]	92	116	271	73
specific surface area (BET) [m ² /g]	32.56	13.37	8.82	14.08
surface tension of 2 vol % suspension [mN/m]	72.5 ± 0.4	71.5 ± 0.2	71.1 ± 0.1	65.3 ± 0.1
IEP at pH	1.2	9.1	5.1	5.8
Hamaker constant [10 ⁻²⁰ J]	1.6	6.7	26 (rutile)	13

^a The surface tension of double deionized water is 72.8 ± 0.2 mN/m.

TABLE 2: Protein Data of Lysozyme (LSZ) and Bovine Serum Albumin (BSA)

protein	mol wt [kDa]	dimensions [nm ³]	isoelectric point at pH	surface tension [mN/m]
LSZ ²¹	14.3	3 × 3 × 4.5	11	60.8 ± 0.2
BSA ²²	66.462	5 × 5 × 9	4.7–4.9	56.0 ± 0.1

content was prepared. The protein concentration was normalized to the specific surface area of the powders (see Table 1). Protein amounts corresponding to theoretical surface concentrations of 0, 25, 50, 100, 200, 400, and 800 ng/cm² were dissolved in 5 mL double deionized water and added to the oxide suspensions. This water amount was taken into account for the 2 vol % suspension preparation.

The protein treated suspensions were equilibrated in bottles with fastened lids under stirring conditions at 25 °C for 16 h. The pH was in all cases around 7.5 ± 0.5.

2.2.2. ζ Potential. The ζ potentials of the oxide suspensions were measured using the electroacoustic Colloidal Vibration Current (CVI) technique (DT 1200, Dispersion Technology) with a built-in titration unit. This method characterizes the ζ potential by means of a probe that uses ultrasound as a driving force for generating an electroacoustic effect. The electroacoustic effect is used to compute the ζ potential of the particles applying electroacoustic theory.²⁴ Proteins in solution are invisible to this

method due to the very small difference in density between the protein and water. Only proteins adsorbed to solid particles with densities > 1 g/cm³ can be detected by this technique. The ζ potentials were measured for all oxide suspensions after 16 h of equilibration time. More details regarding the measurement procedure can be found elsewhere.²⁵

The supernatants of all oxide powders treated with proteins were obtained by centrifugation. The electrical conductivities of the supernatants were correlated with values found for KCl in the literature.²⁶ All measured conductivities corresponded to ionic strengths of 0.5 mM KCl and below.

2.2.3. Determination of the Adsorbed Protein Amount by UV/Vis Spectroscopy. To determine the amount of surface adsorbed protein, four 1.5 mL samples were withdrawn from each suspension at pH 7.5 ± 0.5 after 16 h and placed in plastic centrifuge cuvettes. Subsequently, the cuvettes were centrifuged for 10 min at 3800 g in an Eppendorf 5417R table centrifuge thermostated at 25 °C. The supernatants were transferred to fresh cuvettes and centrifuged again. The protein concentrations of these supernatants were measured by using the Bradford method.²³ Following this method, the vis absorption values of the protein samples were measured at a wavelength of 595 nm, using an UV/vis spectrometer (Lambda 2, Perkin-Elmer). The results were compared to reference curves for the specific protein

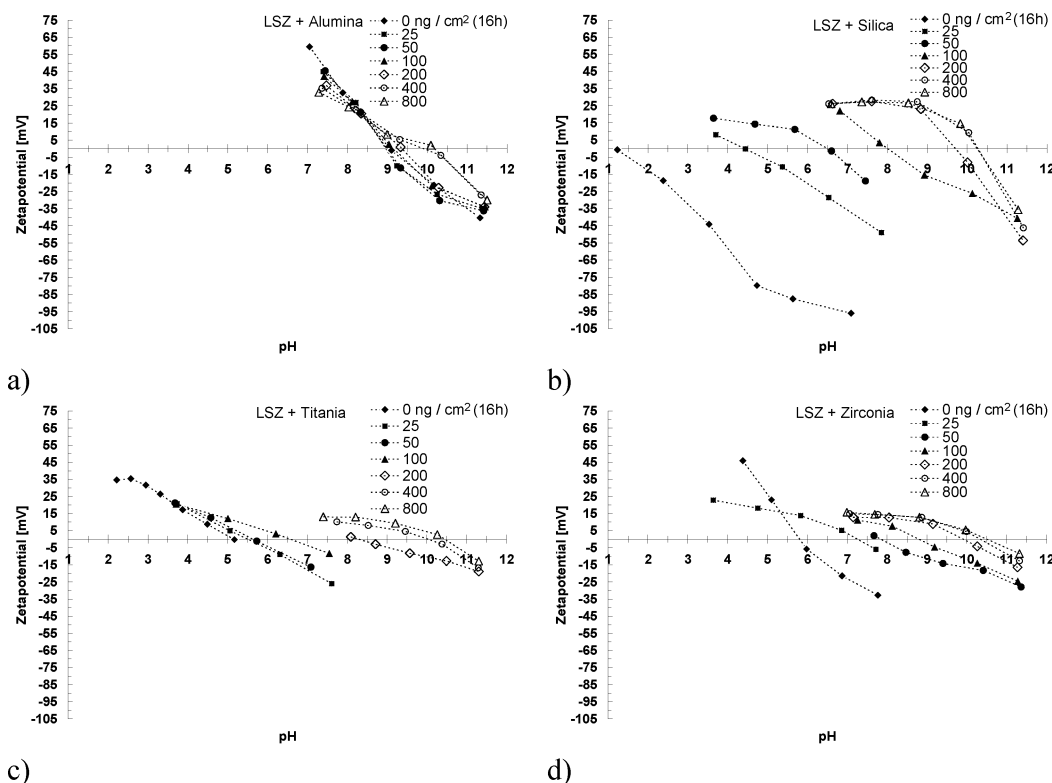


Figure 1. ζ potential curves measured for LSZ treated aqueous oxide suspensions after 16 h of adsorption time at pH 7.5 ± 0.5. Protein concentrations are normalized to the oxide surface area.

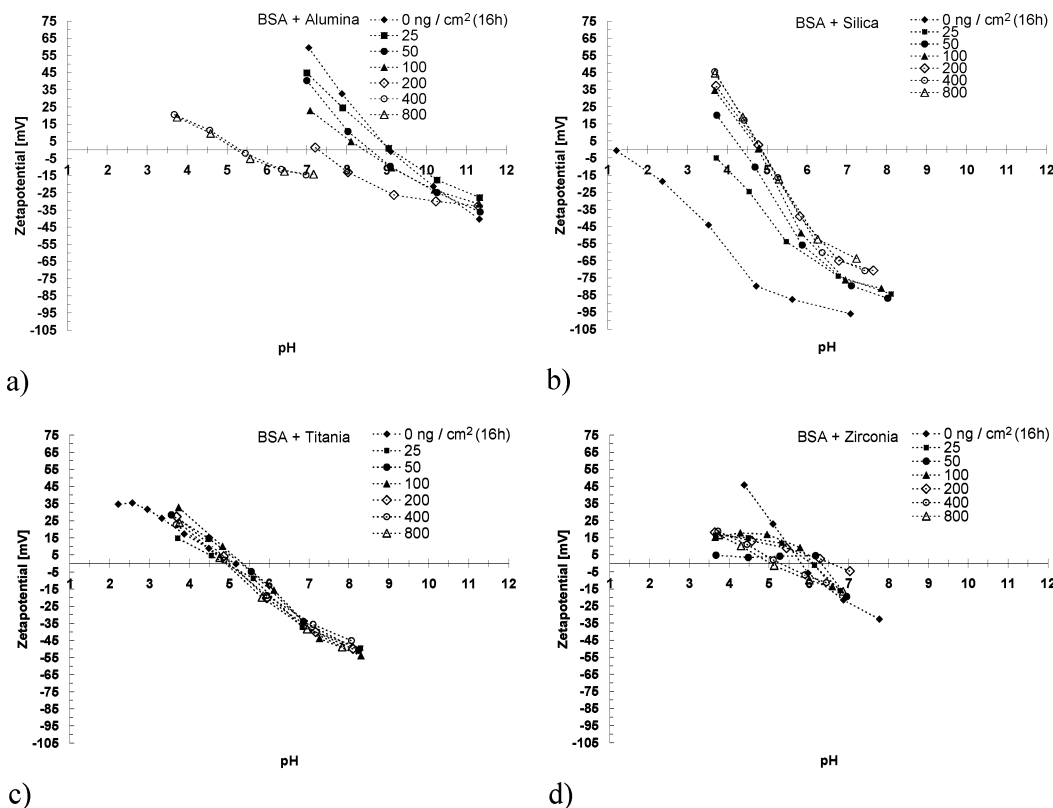


Figure 2. ζ potential curves measured for BSA treated aqueous oxide suspensions after 16 h of adsorption time at pH 7.5 ± 0.5 . Protein concentrations are normalized to the oxide surface area.

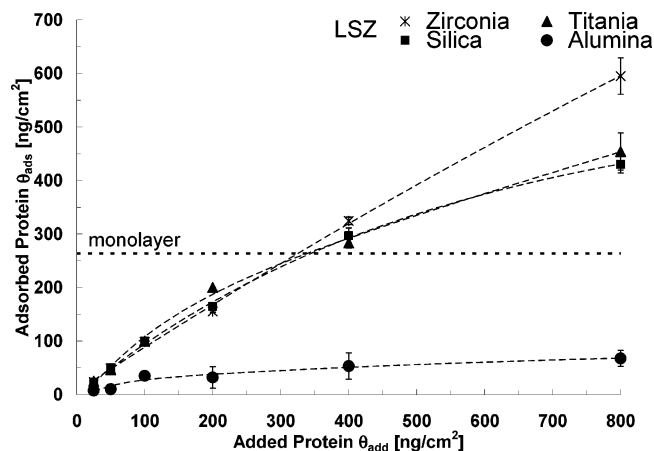


Figure 3. Isothermal adsorption curves after 16 h of adsorption time at pH 7.5 ± 0.5 for LSZ on different oxides. ZrO_2 adsorbs the highest and Al_2O_3 the smallest total amount. The dotted horizontal line indicates the LSZ amount needed for a monolayer formation. The curve fits are for guiding the eyes only.

TABLE 3: pH Values for Maximum IEP Shift

	SiO_2	Al_2O_3	TiO_2	ZrO_2
LSZ	10.3	10.2	10.4	10.5
BSA	4.9	5.2	4.9	5

with a lowest detection limit of 0.007 mg/mL. Typical protein concentrations added to the oxide suspensions were 0.2 mg/mL and higher. The adsorbed amount of protein was calculated from the protein concentration left in the supernatant and the total amount of protein added in the beginning.

3. Results

3.1. ζ Potential and IEP. In Figures 1 and 2 the ζ potential values measured vs pH are plotted for the oxide suspensions

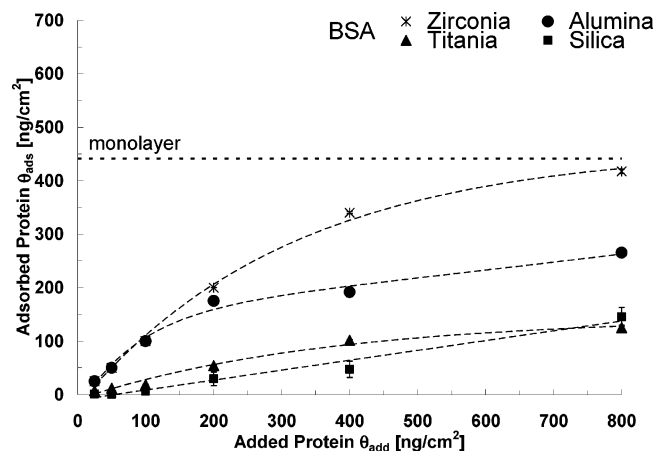


Figure 4. Isothermal adsorption curves after 16 h of adsorption time at pH 7.5 ± 0.5 for BSA on different oxides. ZrO_2 adsorbs the highest and SiO_2 the smallest total amount. The dotted horizontal line indicates the BSA amount needed for a monolayer formation. The curve fits are for guiding the eyes only.

treated with different concentrations of LSZ and BSA after 16 h of equilibration time. Titrations were always started at pH 7.5 ± 0.5 . A general trend can be observed for all protein treated oxide suspensions: The IEP shifts toward the corresponding IEP of the added protein. For LSZ, the IEPs shift toward pH 11 and for BSA toward pH 5. The pH values obtained for the maximum IEP shift are summarized in Table 3. For titania the ζ potential curves hardly change after BSA treatment. The same applies for the ζ potential curves for zirconia treated with BSA and alumina treated with LSZ.

3.2. Adsorbed Protein Amount. Isothermal adsorption curves for 16 h of equilibration time at 25 °C are given in Figures 3 and 4, normalized to the powder surface area. Zirconia

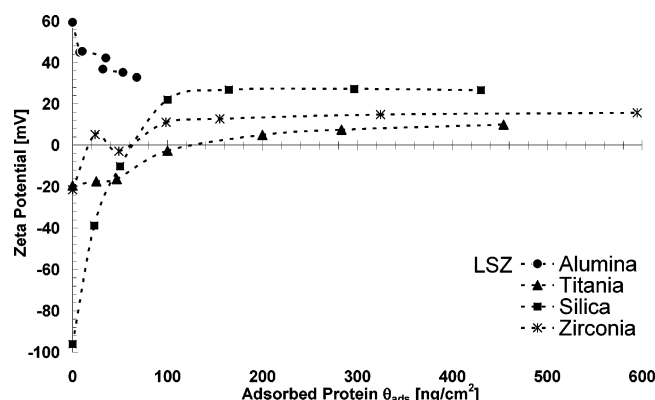


Figure 5. ζ potential plotted vs adsorbed LSZ amount after 16 h of adsorption time at pH 7.5 ± 0.5 . The error bars are not included for clarity reasons (see Figure 3).

shows the highest total adsorbed protein amount for both proteins. Silica and titania adsorb about the same amount of BSA and LSZ. Alumina adsorbs much less LSZ than silica and titania (see Figure 3). In contrast, alumina adsorbs significantly more BSA than silica and titania (see Figure 4).

For LSZ, the required protein amount for a theoretical monolayer formation was exceeded in the cases of zirconia, titania, and silica. Only alumina did not reach the monolayer limit (Figure 3). For BSA, none of the oxides reached a monolayer for the investigated protein concentrations except for zirconia (Figure 4).

The required protein amount for forming a monolayer was calculated by using the molecular weights and smallest dimensions given in Table 2 assuming tight packing. For BSA we obtain 441 ng/cm² and for LSZ 263 ng/cm².

3.3. ζ Potential vs Adsorbed Protein. Figures 5 and 6 show the ζ potential vs adsorbed protein amount (θ_{ads}) obtained at pH 7.5 ± 0.5 . These graphs result from the combination of the ζ potential curves and the protein adsorption curves (Figure 1 to Figure 4). For LSZ (Figure 5), alumina requires the smallest adsorbed protein amount of 32 ng/cm² to reach a stable ζ potential value within ± 5 mV. The other oxides require an adsorbed protein amount of about 100 ng/cm² to reach a level-off value.

In the case of BSA (Figure 6), silica and titania reach first a stable ζ potential value at around 20–30 ng/cm². For alumina, the level-off value is not reached until 190 ng/cm².

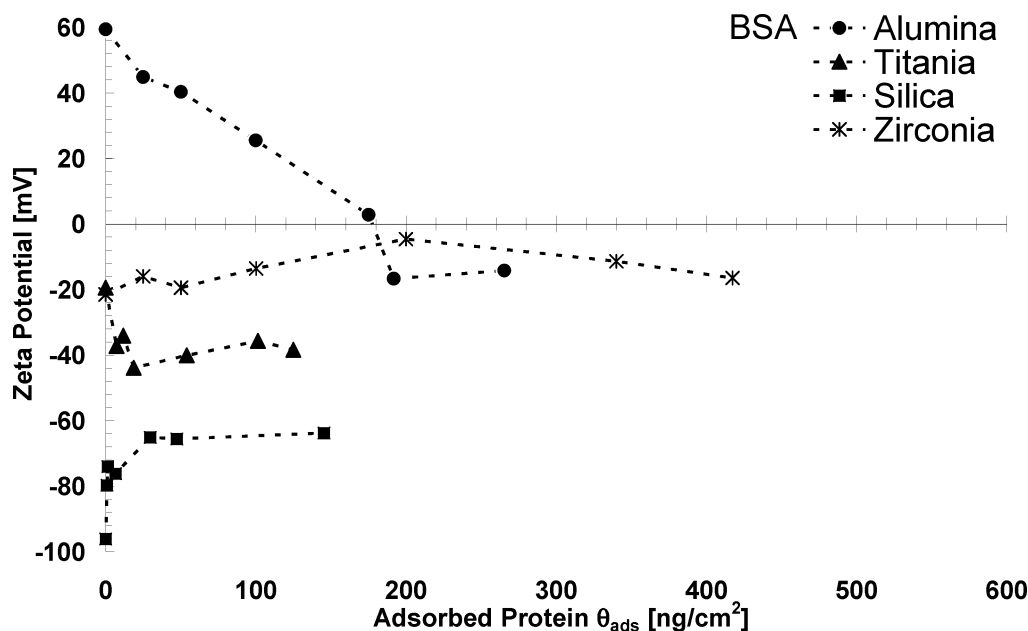


Figure 6. ζ potential plotted vs adsorbed BSA amount after 16 h of adsorption time at pH 7.5 ± 0.5 . The error bars are not included for clarity reasons (see Figure 4).

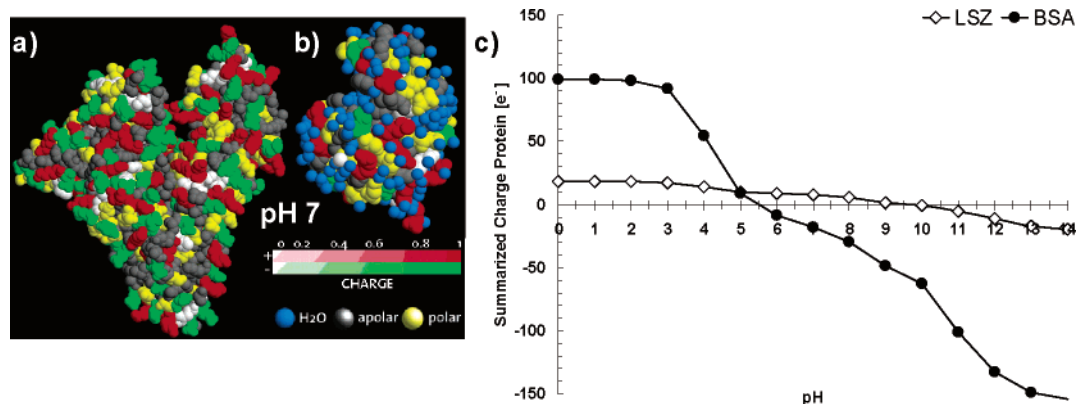


Figure 7. Calculated spatial protein charge distributions of HSA (a) and LSZ (b) at pH 7. Structure files were taken from the protein data bank.³⁰ White spheres are amino acids which are not charged at pH 7. In panel c the summarized charge curves are plotted for both proteins. The calculated IEP of BSA is at pH 5.5 (using the actual amino acid sequence) and that of LSZ is at pH 9.5.

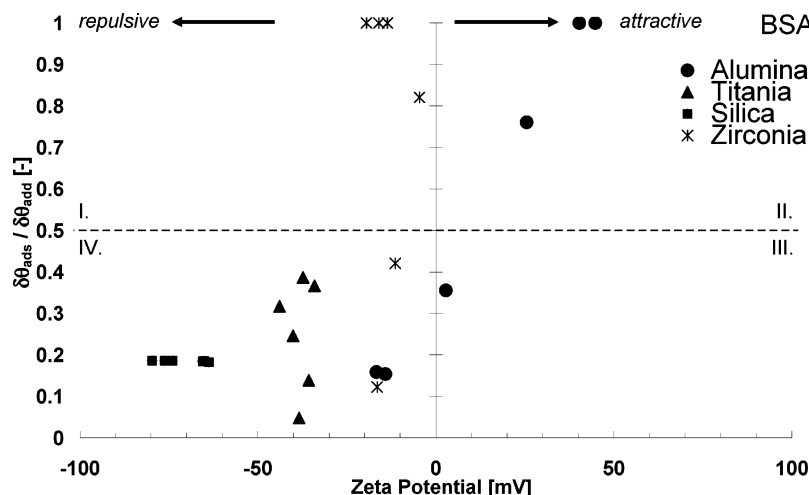


Figure 8. $\delta\theta_{\text{ads}}/\delta\theta_{\text{add}}$ (slopes of the curves in Figure 4) plotted vs the ζ potential for BSA at pH 7.5 ± 0.5 . The dotted horizontal line is at $\delta\theta_{\text{ads}}/\delta\theta_{\text{add}} = 0.5$. Most of the data points are found in quadrants II and IV (except for zirconia).

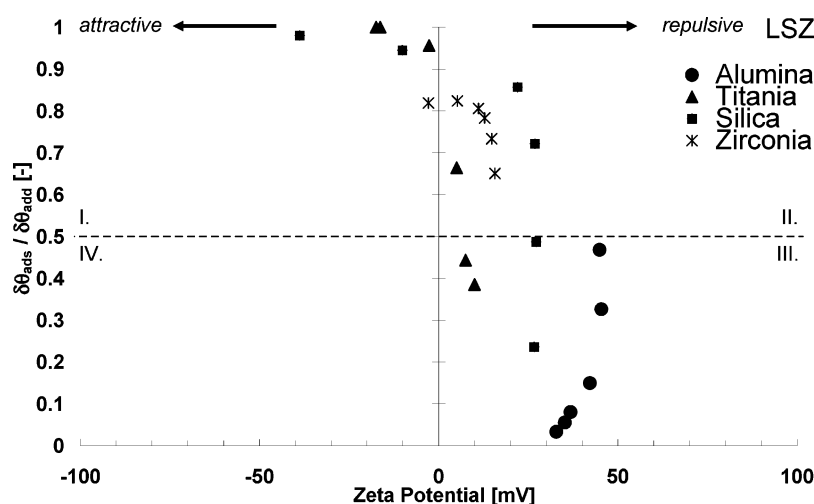


Figure 9. $\delta\theta_{\text{ads}}/\delta\theta_{\text{add}}$ (slopes of the curves in Figure 3) plotted vs the ζ potential for LSZ at pH 7.5 ± 0.5 . The dotted horizontal line is at $\delta\theta_{\text{ads}}/\delta\theta_{\text{add}} = 0.5$. Most of the data points are found in quadrants I and III (except for zirconia).

4. Discussion

4.1. ζ Potential and Protein Amount Adsorbed. All the IEPs of the protein treated oxide suspensions were shifted to the IEPs of the adsorbed proteins. LSZ did not change the ζ potential and IEP of alumina significantly, only at high concentrations (400 and 800 ng/cm²) could an effect be observed (Figure 1 a). A similar effect was observed for titania and zirconia. The IEP and the ζ potential hardly changed over the titrated pH range for all BSA concentrations (Figure 2c,d). Silica, which is also negatively charged at pH 7.5, shows a significant change of the ζ potential curves after BSA treatment (Figure 2b). The reason for the indifference of the titania and zirconia ζ potential curves to BSA adsorption seems to lie in the IEPs of titania and zirconia (at pH 5.1 and 5.8), which are very close to that of BSA (at pH 4.7–4.9). The same reasoning applies to LSZ-treated alumina suspensions.

Comparing the adsorbed protein amounts at different concentrations at pH 7.5 ± 0.5 , a correlation of the sign of oxide surface charge and the adsorbed protein amount can be found. Higher amounts of protein adsorption are found for oppositely charged particle/protein combinations compared to alike charged surfaces. This holds for alumina, silica, and titania. Alumina (+) adsorbs considerably less LSZ (+) than silica (–) and titania (–) (Figure 3). On the other hand alumina (+) adsorbs much more BSA (–) than silica (–) and titania (–) (Figure 4).

Zirconia does not follow this scheme. Even though the zirconia surface is negatively charged, like BSA at pH 7.5, it adsorbs the highest amount of BSA (Figure 4). Another driving force seems to play a more important role than electrostatic attraction/repulsion. van der Waals attraction is unlikely to be the reason as titania has a two times higher Hamaker constant than zirconia (Table 1). Despite the higher Hamaker constant, titania does not adsorb as much BSA while having a negative surface charge at pH 7.5 ± 0.5 similar to zirconia.

However, the comparison of the surface tensions obtained for 2 vol % aqueous oxide suspensions in Table 1 shows that the zirconia suspension has a measurable lower surface tension at the air interface (65 mN m^{–1}) than the other investigated oxides and water (~ 71 –73 mN m^{–1}). As air is considered to be hydrophobic, a lower surface tension indicates a higher overall hydrophobicity for the zirconia suspension. From contact angle measurements²⁷ zirconia was also found by others to be less hydrophilic than, e.g., silica. Because proteins are partly composed of amino acids which are hydrophobic, hydrophobic interaction could be a reason for the considerable amount of BSA adsorbed on zirconia despite the repulsive ζ potential. Between the two proteins, BSA is overall less hydrophilic than LSZ as it can be derived from surface tension measurements of protein solutions (Table 2) and from literature.²¹

It should be noted that the ζ potential values are approximations and not absolute values as the protein layer thicknesses are not exactly the same for all measurements, affecting the electrophoretic mobility as discussed by Ohshima.²⁸

4.2. Change of ζ Potential and Electrostatic Attraction/Repulsion. Comparing the change of ζ potential vs the adsorbed protein amount for silica, alumina, and titania (Figures 5 and 6) it can be seen that BSA and LSZ adsorb on oxide surfaces which are of the same charge, e.g., BSA/silica. Also for BSA/alumina adsorption the ζ potential eventually changes its sign and protein adsorption can still be measured.

We can calculate the charge distribution for each protein by summing up all amino acids that carry charges taking into account their dissociation ratios for different pHs according to refs 25 and 29. The spatial protein charge distributions for BSA and LSZ are illustrated by Figure 7a,b at pH 7. The X-ray structure files were taken from the online protein data bank.³⁰ For BSA the HSA file was used as in ref 25. Figure 7c shows the sum curve for both proteins as a function of pH. One BSA molecule carries many more charges than a LSZ molecule. For the charge calculation the actual BSA primary sequence was taken from ref 31. From Figure 7 it can be seen that a net charge curve is not enough to describe the protein charge distribution.

To compare the adsorption of both proteins and the correlation with the particle ζ potentials, Figures 8 and 9 show the slopes $\delta\theta_{\text{ads}}/\delta\theta_{\text{add}}$ from Figures 3 and 4 plotted vs the measured ζ potential. The repulsive and attractive protein–oxide interface regions are indicated for BSA and LSZ. The figures are subdivided into four quadrants I–IV by drawing a horizontal line at $\delta\theta_{\text{ads}}/\delta\theta_{\text{add}} = 0.5$.

For BSA adsorption (Figure 8) it can be seen that besides the data points of zirconia all other points are either in quadrant II (attractive ζ potential, high adsorption amount $\delta\theta_{\text{ads}}/\delta\theta_{\text{add}} > 0.5$) or IV (repulsive ζ potential, low adsorption amount $\delta\theta_{\text{ads}}/\delta\theta_{\text{add}} < 0.5$). It can be concluded that for BSA adsorption on alumina, silica, and titania the electrostatic interaction plays a very important role. BSA adsorption data points for zirconia are in the I and IV quadrant and do not seem to be governed by electrostatic interaction only.

For LSZ (Figure 9) most of the data points are situated in quadrants I (attractive ζ potential, high adsorption) and III (repulsive ζ potential, low adsorption) if zirconia is not considered. Also for LSZ electrostatic interaction does apparently govern the protein adsorption process for the investigated oxides, excluding zirconia.

In summary, electrostatic interaction seems to govern protein adsorption for the cases where the protein and the materials surface are very hydrophilic (alumina, silica, and titania). For slightly less hydrophilic material surfaces, hydrophobic interaction seems to play an important role in the adsorption process as well and can even overcome electrostatic repulsion as found for protein adsorption on zirconia.

5. Conclusions

The ζ potentials and IEPs were measured for alumina, silica, titania, and zirconia and correlated with the protein amount adsorbed at pH 7.5. It was found that zirconia adsorbs the

highest protein amount even under repulsive electrostatic conditions in the case of BSA. One reason could be the less hydrophilic zirconia particle surface. For the other oxides, which are very hydrophilic, it was found that electrostatic interaction determines the amount of adsorbed protein.

The ζ potential curves in this study serve to estimate the sign of the surface charge and the ζ potentials of protein treated oxide surfaces for different pHs for biomedical applications and to support other techniques evaluating protein adsorption such as OWLS and QCM. The presented data are comprehensive and can be valuable in refining and testing different protein adsorption models.

Acknowledgment. We thank Dr. L. P. Meier and Prof. Dr. M. Textor for helpful discussions, M. Rezwan for the SDS-PAGE analysis, and ETH Zurich for funding this project (TH Fund No. 0-20-148-03).

References and Notes

- (1) Hook, F.; Voros, J.; Rodahl, M.; Kurrat, R.; Boni, P.; Ramsden, J. J.; Textor, M.; Spencer, N. D.; Tengvall, P.; Gold, J.; Kasemo, B. *Colloids and Surfaces B: Biointerfaces* **2002**, *24*, 155.
- (2) Roth, C. M.; Sader, J. E.; Lenhoff, A. M. *J. Colloid Interface Sci.* **1998**, *203*, 218.
- (3) Servagent-Noinville, S.; Revault, M.; Quiquampoix, H. *J. Colloid Interface Sci.* **2000**, *221*, 273.
- (4) Urano, H.; Fukuzaki, S. *J. Biosci. Bioeng.* **2000**, *90*, 105.
- (5) Adamczyk, Z. *Adv. Colloid Interface Sci.* **2003**, *100–102*, 267.
- (6) Jonsson, B.; Stahlberg, J. *Colloids Surf., B* **1999**, *14*, 67.
- (7) Hemar, Y.; Horne, D. S. *J. Colloid Interface Sci.* **1998**, *206*, 138.
- (8) Barroug, J.; Lemaitre, A.; Rouxhet, P. G. *Colloids Surf.* **1989**, *37*, 339.
- (9) Norde, W.; Rouwendal, E. *J. Colloid Interface Sci.* **1990**, *139*.
- (10) Kondo, A.; Mihara, J. *J. Colloid Interface Sci.* **1996**, *177*, 214.
- (11) Norde, W.; Lyklema, J. L. *J. Colloid Interface Sci.* **1978**, *66*, 266.
- (12) Norde, W.; Lyklema, J. L. *J. Colloid Interface Sci.* **1978**, *66*, 257.
- (13) Norde, W.; Lyklema, J. L. *J. Colloid Interface Sci.* **1978**, *66*, 285.
- (14) Katti, K. S. *Colloids Surf., B* **2004**, *39*, 133.
- (15) Kosmulski, M.; Egon, M. *Colloids Surf.* **1992**, *64*, 57.
- (16) Parks, G. A. *Chem. Rev.* **1965**, *65*, 177.
- (17) Loglio, G.; Pandolfini, P.; Miller, R.; Makievski, A. V.; Ravera, F.; Ferrari, M.; Liggieri, L. Drop and bubble shape analysis as tool for dilational rheology studies of interfacial layers. In *Novel Methods to Study Interfacial Layers*; Möbius, D., Miller, R., Eds.; Elsevier: Amsterdam, The Netherlands, 2001; Vol. 11, p 439.
- (18) Israelachvili, J. *Intermolecular & Surface Forces*, 2nd ed.; Academic Press: London, UK, 1991.
- (19) Ackler, H. D.; French, R. H.; Chiang, Y.-M. *J. Colloid Interface Sci.* **1996**, *179*, 460.
- (20) Laemmli, U. K. *Nature* **1970**, *227*, 680.
- (21) Burton, W. G.; Nugent, K. D.; Slattery, T. K.; Summers, B. R.; Snyder, L. R. *J. Chromatogr. A* **1988**, *443*, 363.
- (22) Carter, D. C.; Ho, J. X. *Adv. Protein Chem.* **1994**, *45*, 153.
- (23) Bradford, M. M. *Anal. Biochem.* **1976**, *15*, 248.
- (24) *Studies in Interface Science*; Dukhin, A. S., Goetz, P. J., Eds.; Elsevier: Amsterdam, The Netherlands, 2002; Vol. 15.
- (25) Rezwan, K.; Meier, L. P.; Rezwan, M.; Vörös, J.; Textor, M.; Gauckler, L. J. *Langmuir* **2004**, *20*, 10055.
- (26) *CRC Handbook of Chemistry and Physics*, 83rd ed.; Lide, D. R., Ed.; CRC Press: Boca Raton, FL, 2002.
- (27) van Oss, C. J.; Wu, W.; Giese, R. F.; Naim, J. O. *Colloids Surf., B* **1995**, *4*, 185.
- (28) Ohshima, H. *J. Colloid Interface Sci.* **2000**, *228*, 190.
- (29) Biesheuvel, P. M.; Stroeve, P.; Barneveld, P. A. *J. Phys. Chem. B* **2004**, *108*, 17660.
- (30) RCSB Protein Data Bank; Vol. 2004.
- (31) Hirayama, K.; Akashi, S.; Furuya, M.; Fukuhara, K. *Biochem. Biophys. Res. Commun.* **1990**, *173*, 639.